SHAPE FROM SHADING FOR SURFACES WITH TEXTURE AND SPECULARITY

by

E. North Coleman Jr. and Ramesh Jain

Department of Computer Science
Wayne State University
Detroit MI 48202

ABSTRACT

The primary focus of this work is to experimentally explore a method for determining three dimensional surface shape from intensity information. A method is developed. using existent theory, for determining the shape of visually textured surfaces exhibiting varying degrees of specularity. The photometric stereo is extended to four source photometry as the basis for this work. The reflectance map approach for determining surface normals is shown to be of little value in this context and a more direct method of computing these normals is used.

1 INTRODUCTION

Several methods are available for obtaining depth information for surfaces. These methods are divided into what Woodham [8] refers to as direct methods and indirect methods. Direct methods try to measure range (distance) directly. Indirect methods attempt to determine distance by measuring parameters calculated from images of the illuminated object.

One indirect method for obtaining surface shape is by analysis of the radiometry of image formation[1-5,7-9l. Commonly known as shape from shading, this method can be applied wherever the direction of incident illumination is known and/or can be controlled. It is this technique which is the subject matter of this paper.

Horn [1] showed how shape could be determined by solving non-linear, first order partial differential equations to find components of the surface gradient. While the gradient could not be determined locally, numerical integration of the equations permitted characteristic curves to be traced out on the object surface. Woodham [8,9] suggested photometric stereo for locally determining surface gradients using multiple sources of illumination.

Multiple source photometry is usually implemented using one reflectance map for each image. To initialize such a reflectance map, the system is calibrated using a sphere having a constant surface reflectance factor. Silver [7] has shown this method to be very effective in solving for shape with uniform matte surfaces.

This work was partially supported by National Science Foundation under the Grant No. MCS-8100148.

Specular reflection, or highlights, appear on a surface when the angle between the viewer and source of illumination is bisected by the surface normal. By producing a mirror- like reflectance off an object's surface, specularity causes measured intensity values to be higher by the magnitude of the specular component. Although attempts have been made to account for specularity in reflectance functions and reflectance maps, these functions are contrived for certain cases and fail to solve the general problem. In this paper, visual texture is considered as a pattern or variance of intensity appearing on an object surface.

The motivation behind this paper is to adapt multiple source photometry to surfaces varying in both specularity and visual texture. Toward this end it will be shown how surface normals can be computed by solving sets of simultaneous linear equations. Detailed by Woodham [9] this method can be used on textured surfaces. Furthermore, it will be shown how a fourth source of illumination can be used to detect specular reflection. Once discovered, the specular component can be removed from the computation of a local normal vector .

11 SURFACE SHAPE FROM INTENSITY

2.1 Definitions

Suppose a surface is defined explicitly by an equation of the form

$$z = F(x.y) \qquad 2.1$$

if we choose to represent surface orientation with normal vectors, the orientation of any point on the surface can be written as

$$N = (Fx, Fy, -1) \qquad 2.2$$

where Fx and Fy are the first partial derivatives of F with respect to x and y, respectively. In all cases, the viewer will be along the negative Z axis compared to the surface being viewed. The surface normal (0,0,-1) points directly at the viewer and is orthogonal to the image plane.

To simplify the geometry we assume that the distance between the viewer and the object being viewed is large in relation to the object's size. This allows us to approximate the perspective-projection of the imaging device by an orthographic projection.

Using two variables p and q, we define

$$p = Fx \quad \text{and} \quad q = Fy.$$

From this, the surface normal of F (x,y) at any point (x,y) can be written as (p,q,-l). The quantity (p,q) is defined as the gradient of F.

A surface photometric function Q(i,e,g) for a single source can be defined in terms of the incident angle (i), emittance angle (e) and phase angle (g). As such, the angles quantify the relationship between the source vector, view vector and surface normal vector. Each of these vectors can be written in gradient space coordinates as

V = (0,0,-1) (view vector) 2.3

S = (ps,qs.-l) (source vector) *2.4*

N = (p,q,-l) (normal vector) 2.5

From the reflectance map, Woodham [8] illustrates how a single intensity value restricts the p and q values of the surface normal to a particular iso-brightness contour. The goal of shape from shading is to isolate which (p,q) value on the contour is the correct surface gradient.

2.2 Single Source Photometry

Once a reflectance map is established, the process of determining the shape of sample objects can begin. When a single source of illumination is used, a single image intensity value maps into many possible surface orientations. To resolve these ambiguities, algorithms developed to solve for surface shape, using a single source, assume certain surface constraints. Woodham [8] assumes surfaces to be uniform, matte, convex and smooth with continous first and second partial derivatives. From this assumption, his iterative algorithm propagates these constraints back and forth until converging on a solution for the entire surface.

2.3 Multiple Source Photometry

Photometric stereo, in essence, is multiple source photometry where two or more images of an object are obtained from the same viewpoint. In each image the object is illuminated from a different direction by a single source. This gives rise to a n-tuple of intensity values for each (x,y) point on the surface.

The first step in multiple source photometry is to establish a reflectance map for each source of illumination. Then by tracing iso-brightness contours for each source/intensity the intersection point for all contours can be found. This intersection point satisfies the intensity value requirements for each source and is thus the surface gradient at the corresponding image point (x.y) .

It has been shown [9] that a minimum of three distinct iso-brightness contours is needed to find the surface gradient for a lambertian surface. This implies a minimum of three sources is needed. For the contours to intersect at single point the source vectors cannot be colinear.

2.4 Limitations of the Reflectance Map

Given any reflectance map, shape can be determined for surfaces having photometric properties identical to the surface used for reflectance map calibration. This implies that the specular component of all sample surfaces must be identical to that cast in the reflectance map. Additionally, specularity cannot be detected, as there is no indicator to show if an intensity value is elevated due to specular reflection. Finally, when establishing a reflectance map the surface reflectance factor R is made constant, for all points on the surface. This forces a uniformity of intensity on the surface and prevents the application of reflectance map techniques to visually textured surfaces.

2.5 A Direct Solution for the Lambertian Surface

To overcome the limitations of reflectance map techniques, a solution for surface shape must provide both the surface normal and surface reflectance factor R at each point. For Lambertian surfaces this is

I (x.y) -R*cos(i) - R*(S.N)/|S||N(2.6

If it is assumed the source and normal vectors, S and N, are unit vectors, the denominator for equation 2.6 becomes 1. Equation 2.6 can now be written:

I (x.y) = R*S.N)

=R* (Sx,Sy.Sz) . (Nx.Ny.Nz) 2.7

where (Sx.Sy.Sz) are the known components of the source vector and (Nx.Ny.Nz) are the unknown components of the surface normal.

Since 2.7 is an equation with three unknowns, a minimum of three sources and associated intensity values is needed to compute the surface normal at each point. Given the sources SI, S2 and S3 along with intensity values II, 12 and 13 at (x,y) a set of simultaneous equations can be formed to solve for N.

|H II [S1x S1y S1z] [Nx]

12 - S2x S2y S2z Ny 2.8

[13] [S3x S3y S3z [Nz]

If we use Ms to symbolize the source matrix, I the intensity feature vector at (x.y) and N the normal vector, equation 2.8 becomes:

I (x.y) - R *[MS]N 2.9

To solve for the reflectance factor, R, and unit normal, N, equation 2.9 can be written as:

R * N - [MS] 7 2.10

Using equation 2.10 the surface normal can be computed directly from a triplet of intensity values I and the inverse of the source matrix Ms. For Ms to have an inverse the source vectors SI, S2 and S3 must not be colinear.

The reflectance factor, R, can be found simply by taking the magnitude of the right side of equation 2.13- This is because the surface normal, N, is of unit length.

R = I [Msj"' 7 I 2.11

Once the reflectance factor is found the unit normal can be computed as:

N - (1/R) *(Ms]' '. 2.12

Using 2.12 all three components of the unit surface normal can be found. It is necessary to compute all three components as the unit surface normal will not necessarily have Nz = - 1 .

2.6 Handling Visual Texture

By solving for the unit normal vector in the previous section, it has also been shown that the surface reflectance factor R can be determined locally at each (x,y) point on a surface. This implies that R need not be constant over the surface. Regardless of how R varies, it can still be computed at each point using equation 2.11.

Visual texture can be thought of as a pattern caused by variance in the surface reflectance factor from point to point on a given surface. Indeed, shading models have been developed in computer graphics utilizing a variable reflectance factor to effect surface intensity[6]. Thus, it can readily be seen that applying equation 2.10 allows surface normals to be computed when the object is visually textured, as R is computed

locally at each point.

2.7 Overcoming Specular Distortion

One method of overcoming specularity problems in a shading model is by incorporating terms into the reflectance function to account for the specular component. Building such terms into the reflectance function, however, ties the model to a single expression of specularity. A more flexible method is needed which enables the specular component to vary from one surface to another or even across the same surface.

As was shown in section 2.5. three sources are all that are needed to uniquely determine surface normals for a Lambertian surface. If, however, a point on the surface is subject to specular reflection from one of the three sources, the computed normal vector will be incorrect due to an elevated intensity value. By adding a fourth source, it becomes possible to compute a set of four surface normal vectors for each point; i.e. one normal for each permutation of three intensity values. It is this redundancy which allows tagging and removal of the specular source.

To see how this is accomplished first assume we are given four measured intensity values nt a point (x.y) on a surface; one intensity from each source/image. If none of the intensities has a specular component, the resulting four surface normals will appear as in Figure la. On the other hand, suppose the intensity value from an arbitrary source/image (source four in this case) contains a specular component elevating its value. The resulting four normals computed will be similar to the case illustrated in Figure lb.

It can readily be seen that there is a greater deviation in both direction and magnitude of the vectors in Fig. lb than those in Fig. la. Three of the normal vectors in Fig. lb (the three computed using source four) are affected by a specular component. Because of this reason, their magnitudes, R, are greater and they are skewed more in the direction of the specular source.

A method can now be developed to eliminate specular effects using a thresholding procedure. The first step is to compute a relative deviation in the surface reflectance factor R at each point on the surface. This can be done using the formul a:

$$Rdev = \left[\sum_{i=1}^{4}(Ri-Rmean)\right] / (4*Rmin) \qquad 2.14$$

where Ri is each reflectance factor computed at (x,y) and Rmin is the smallest of these. A reflectivity deviation map can be displayed for the entire surface showing the reflectance deviation Rdev at each point. On a reflectivity deviation ' map, specular regions will be characterized by high reflectance deviation.

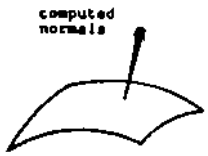

Figure la. Computed normals at a single point on the surface when no specular component is present. Mean deviation among norma IS is small .

When computing surface normals, Rdev at each point is checked against the threshold value Rt. If Rdev at a point is less than or equal to Rt, a specular component is not considered present. The surface normal is computed as the average of all four normals calculated at this point. Rdev greater than Rt indicates a specular contribution at this point from one of the sources. To eliminate this specular component, the surface normal is chosen as the computed normal vector having the smallest reflectance factor.

In practice, the use of a threshold value will allow many surfaces to be analyzed successfully. A limiting factor is that the specular component cannot be so great as to cause specular regions from two or more sources to overlap. This can be overcome to some degree by adjusting the angle of incidence for each source to prevent overlap.

Finally, the phase angles between all source vectors and the view vector must not be so large as to prevent all four sources from contributing measurable intensity values throughout the *arc* of specular reflection. For most cases a phase angle of up to 60 degrees can be used (30 degrees above the image plane) but under special circumstances the optimum source angles may have to be determined experimentally.

111I A WORKING SYSTEM

A system consisting of specialized imaging hardware and a series of computer programs was developed to verify the approach proposed above[10]. The set up used to obtain images for our experiments is described in[I0]. This set up allows us to obtain images for different position of the light sources.

3.1 Picture Digitization

All images were digitized directly using an Eyecom high resolution digitizer. The resulting output was a 480 by 480 array of pixels, each containing an 8 bit gray level code (0-255)- The Eyecom was operated in the linear mode.

Once the images were digitized, they were then processed by a program to generate intensity histograms and intensity contour maps. The contour maps and histograms were used to determine intensity threshold values for object boundaries.

3.2 Surface Normal Generation

Surface normal generation was accomplished by the method detailed in section 2.5. As can be seen by equation 2.12 a triplet of intensity values must be multiplied by the inverse of the source matrix, Ms .

Four source matrices were created, one for each permutation of three source vectors. The inverse for each matrix was computed using

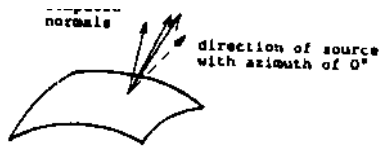

Figure I!>. Computed normals at a single point with source at 0 exhibiting specularity. Intensity value from this source is elevated causing a high deviation among these normals.

Gaussian elimination with partial pivotal condensation.

Computation of the surface normal vectors was very straight forward. Each triplet pf intensity values (11,12,13) at a point (x,y) was multiplied by the appropriate inverse (MI in this case) to give the normal. The normal was reduced to a unit normal and the reflectance factor extracted. Prior to computing the normal, all intensity values had to exceed predetermined threshold levels to insure that the point is on the surface.

As is described in section 2.7. the program determined reflectance deviation at each point on the surface where four normals could be computed. This deviation was then translated into a reflectivity deviation map. From this map we are able to select the maximum deviation allowed between a set of normals at each point.

After the selected deviation threshold is entered, the final normal values are computed. These values represent an average of four vectors if the deviation threshold is not exceeded. Otherwise, the vector corresponding to the lowest reflectance factor is used. All output vectors are unit surface normals to insure correct operation of the depth conversion procedure.

3.3 Depth Conversion

The final step in generating the actual surface is the conversion from surface normals to depth information. That is, for every (x.y) point and normal vector N at (x.y) a 2 value with respect to the image plane must be computed.

First, assume a surface patch as shown in Figure 2. Also assume each of the surface normals NO, NI, N2, N3 is known at the points (0,0), (1,0), (0,1), (1.1) respectively. Finally, a starting 2 value at (0,0) is either chosen or known. To compute 2 values at the remaining three points a function must be chosen to specify how the normal varies along the edges of the patch.

If the points (0,0) and (1,0) are very close relative to surface si2e, the curve between these points can be approximated by its average tangent line. When considering the distance between pixels, this condition holds.

Given the following normal vectors:

N0 = (n0x,n0y,n0z) at (0,0)
N1 = (n1x,n1y,n1z) at (1,0)
N2 = (n2x,n2y,n2z) at (0,1)
N3 = (n3x,n3y,n3z) at (1,1)

we wish to compute z at (1,0) which is along the x axis from (0,0). The tangent line desired passes through the point (0,0,z) and is perpendicular to the average normal between these points. This line can be expressed as:

$$ax+b(z(1,0)-z(0,0)) = 0 \quad 3.1$$

where:

$$a = (n0x+n1x)/2 \quad 3.2$$
$$b = (n0z+n1z)/2 \quad 3.3$$

This gives,

$$z(1,0)=z(0,0)-x(a/b) \text{ with } x=1 \quad 3.4$$

similarly, approximation along the y axis to find z at (0,1) gives:

$$z(0,1)=z(0,0)-y(a/b) \text{ with } y=1 \quad 3.5$$

Here,

$$a = (n0y+n2y)/2 \quad 3.6$$
$$b = (n0z+n2z)/2 \quad 3.7$$

To arrive at z(1,1), two values are computed. One value, z1(1,1) is arrived at by going from (1.0) to (1,1) in the y direction. The second value 22(1,1) is obtained by going from (0,1) to (1.1) along the x direction. The two values are averaged to give 2(1,1).

$$2(1.1) = (z)\ (I, I)+z2\ (1.\ I))/2$$

Z values can also be computed going along the negative x and y directions if a -1 is substituted for x and y in equations 3-4 and 3-5 respectively. This is useful if the value of 2 at (1,1) is known and the 2 values at the other three points are to be computed.

The algorithm for depth conversion begins by choosing an arbitrary 2 value for the point in the center of the image. Next, 2 values are determined at all points along the x and y axes passing through this center point. Finally. 2 values are computed for the remaining points. The final 2 values are offset as necessary to make Z min = 0 (minimum 2 value) .

3.4 Results

Four objects, as shown in Figure 3, were chosen to determine the system's capabilities with actual images. All four objects were made of wood, finished naturally with varnish. The surfaces were thus visually textured (wood grain) with varying degrees of specularity.

Before normals were computed, a reflectivity deviation map was printed for each object. These maps were examined and a threshold deviation code of 'C' was chosen as the maximum deviation allowable for all cases. From these maps, four high deviation areas were identified on the sphere and spheroid surfaces. These areas result from specular reflections from each of the sources. On the other hand, the truncated cone and pyramid show specularity only along the edge points. This is as was expected, for the surfaces of these objects were not inclined at the proper angle for specular reflection.

The plotted results for each object can be seen in Figures 4 through 7- Theses plots show how the essential characteristics of each surface were preserved; each object can be readily

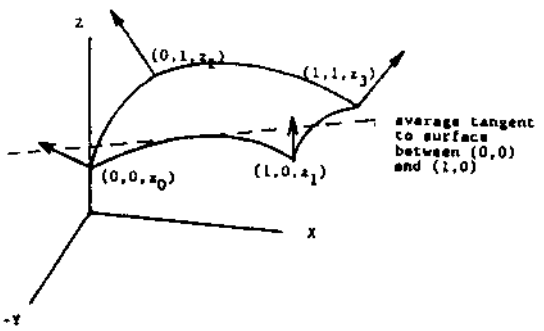

Figure 2. Surface patch and normal vectors. Approximation to surface between (x,y) points (0,0) and (1,0) can be made by using the average tangent line if points are sufficiently close.

Figure 3. Sample objects for experiment:

(a) sphere;
(b) oblate speroid;
(c) truncated cone;
(d) square pyramid.

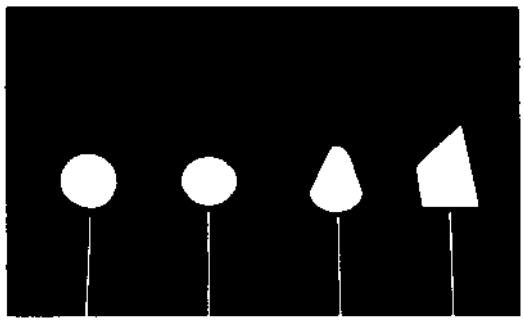

identified. This achieved the fundamental objective of this experiment.

On the plotted surfaces of the sphere and spheroid, valleys or dips are visible. These dips are due mainly to the non-uniformity of the light source. That is, a flat white disk placed under the scanner did not register a constant intensity at all points. These surface irregularities are not sufficient to cause the surfaces to be unrecogni zable.

The sphere and spheroid surfaces do show profile differences when overlayed, the spheroid being more squat. There was not enough intensity information near the horizon, however, to generate the portions of these surfaces where they differ the most.

The cone and pyramid gave excellent results. Of particular interest is edge definition and uniformity on the faces. All planar surfaces have distinct edges and constant surface orientations. Algorithms, using interpolation or iteration, tend to round these edges and hence are best suited to smoothly curved surfaces.

Profile comparisons between actual objects and the generated surfaces indicated the plotted surfaces were somewhat squat. It is felt that this effect resulted because the camera distance was not large enough with respect to object size. The perspective projection of the imaging device was thus too pronounced to effectively be approximated by an orthographic projection. In all cases, however, the results were very promising and demonstrated the method's ability to handle visually textured, specular objects.

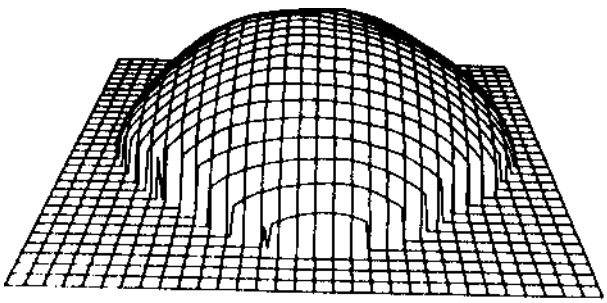

Figure 4. Sphere plotted results. Surface generated from measured intensity values. Viewpoint coordinates: (5,-15,15).

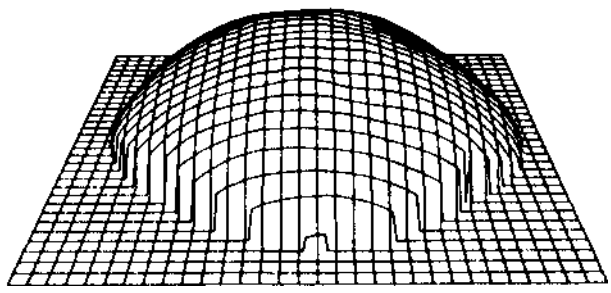

Figure 5. Oblate spheroid plotted results. Surface generated from measured intensity values. Viewpoint coordinates: (5,-15,15).

Figure 6. Truncated cone plotted results. Surface generated from measured intensity values. Viewpoint coordinates: (-15,5,15).

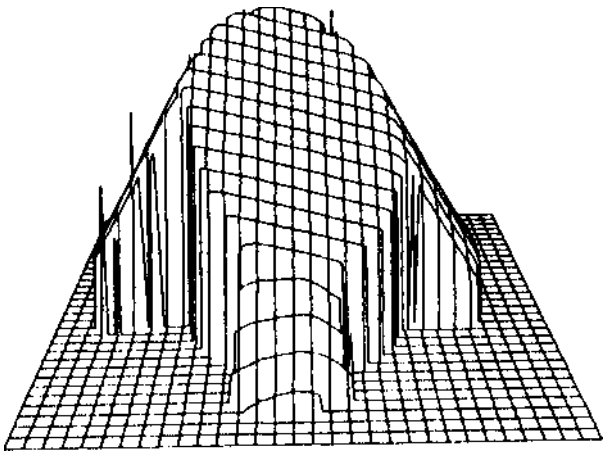

Figure 7. Square pyramid plotted results. Surface generated from measured intensity values. Viewpoint coordinates: (- 15,-15,15).

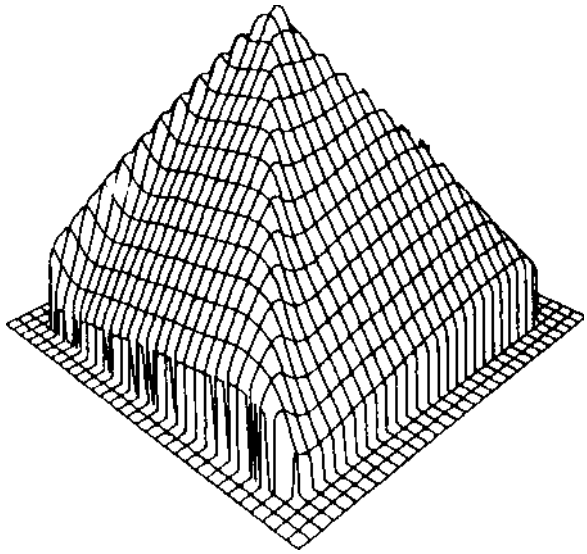

IV CONCLUSION

In this paper we have attempted to contribute to the evolution of the photometric approach for surface shape determination in presence of texture and specularity. As a measure of its effectiveness, the results of this approach are most encouraging. It is hoped that this paper will prove useful in helping to apply shape from shading to surfaces previously thought to be beyond the scope of photometric methods.

REFERENCES

1. Horn, B. K. P., "Obtaining Shape from Shading Information", in The Pyschology of Computer Vision, P.H. Winston (ed.), McGraw-HilT" 1975-

2. Horn, B. K. P., "Image Intensity Understanding". Al Memo 335, M.I.T. A! Laboratory, August 1975.

3. Horn, B. K. P., "Sequins and Quills Representations for Surface Topography", Al Memo 536, M.I.T. Al Laboratory, May 1979-

4. Horn, B. K. P. And Sjoberg, R. W., "Calculating the Reflectance Map", Al Memo 498, M.I.T. Al Laboratory, October 1978.

5. Ikeuchi, K. And Horn, B. K. P., "An Application of the Photometric Stereo Method", Al Memo 539, M.I.T. Al Laboratory, August 1979.

6. Newman W. M. And Sproull R. F., Principals of Interactive Computer Graphics, McGraw-Hi 1 l, New York. 1979.

7. Silver, W. M., "Determining Shape and Reflectance Using Mutiple Images", M.S. Thesis, M.I.T. Al Laboratory, May 1980.

8. Woodham, R. J., "Reflectance Map Techniques for Analyzing Surface Defects in Metal Castings", AI-TR-457. M.I.T. Al Laboratory, June 1978.

9. Woodham, R. J., "Photometric Method for Determining Surface Orientation from Multiple Images", in Optical Engineering, Vol 19. No.l, pp. 139-144, Jan/Feb 1980,

10. Coleman, E. N. And Jain, r., " Obtaining 3-Dimensional shape of textured and specular surfaces using four source photometry ", TR No CSC-81-O2O, Dept. Of Computer Science, Wayne State University. Detroit, MI 48202, April 1981.